9. Noon of the day on which the vaginal plug was detected was considered as E0.5 in the timing of embryo collection.
10. E. N. Meyers and G. R. Martin, data not shown.
11. In 11 of these 50 embryos the liver was abnormally symmetrical, and the spleen, which is normally found on the left, was absent or small. In 2 of these 11 embryos the direction of bowel rotation was reversed. In another 4 of these 50 embryos the liver and spleen appeared morphologically normal, but stomach and spleen situs were reversed. In all embryos with right pulmonary isomerism, and 28 others, a variety of heart abnormalities were detected, including malposition of the cardiac outflow tracts and other vascular vessels.
12. S. P. Oh and E. Li, *Genes Dev.* **11**, 1812 (1997).
13. In normal embryos, Nodal expression is transiently detected in the left LPM beginning at the 2 to 3 somite stage (*17*). Lefty2 RNA is also detected in the left LPM of normal mouse embryos at early somite stages (*15*). Pitx2 RNA is normally detected in the left LPM, but beginning slightly later and persisting longer than Nodal or Lefty2 expression (*5*).
14. Ndl^{lacZ} is an allele in which a *lacZ* gene disrupts the Nodal gene and functions as a reporter for Nodal expression (*17*). $Fgf8^{-/+}$;$Ndl^{lacZ/+}$ animals have normal situs, indicating that double heterozygosity for loss-of-function alleles of *Fgf8* and *Ndl* does not cause any abnormalities in LR asymmetry. These results contrast with the finding of genetic interactions in double heterozygotes for Ndl^{lacZ} and a null allele of either *Smad2* [M. Nomura and E. Li, *Nature* **393**, 786 (1998)] or *Hnf3*β (*25*).
15. C. Meno *et al.*, *Nature* **381**, 151 (1996); C. Meno *et al.*, *Genes Cells* **2**, 513 (1997).
16. Detected by whole-mount RNA in situ hyridization carried out with the protocol described by A. Neubüser, H. Peters, R. Balling, and G. R. Martin [*Cell* **90**, 247 (1997)].
17. J. Collignon, I. Varlet, E. J. Robertson, *Nature* **381**, 155 (1996).
18. Embryos were isolated at the 0 to 2 somite stage (~E8.0), and a heparin bead (H5263, Sigma) soaked in phosphate-buffered saline (PBS) containing bovine serum albumin (BSA, 1 mg/ml) (control BSA-bead) or in PBS-BSA with FGF8 (1 mg/ml) (b isoform; R&D Systems, Minneapolis, MN) (FGF8-bead) was inserted into the right LPM lateral to the node. After 1 hour in stationary culture, the embryos were incubated for 6 to 8 hours in a rotary culture apparatus, as described by K. Sturm and P. Tam [*Methods Enzymol.* **225**, 164 (1993)]. During the culture period the embryos developed to the 4 to 8 somite stage. After culture, the embryos were washed in PBS, fixed, and assayed for β-Gal activity as described (*17*). Ectopic nodal expression was detected in tissue near the bead in 11 out of 18 embryos with FGF8-beads, and in 1 out of 7 embryos with control beads. The Nodal expression domain appeared normal in two embryos with FGF8-beads implanted in the left LPM. No ectopic Nodal expression was detected in 22 embryos isolated at the 4 to 8 somite stage, after implantation of an FGF8-bead in the right LPM and culture as described above.
19. E. N. Meyers and G. R. Martin, unpublished observations.
20. S. Nonaka *et al.*, *Cell* **95**, 829 (1998).
21. C. Chiang *et al.*, *Nature* **383**, 407 (1996).
22. S. Izraeli *et al.*, *Nature* **399**, 691 (1999). Bilateral expression of Nodal was detected in $Shh^{-/-}$ embryos at a much higher frequency than reported here. This might be due to differences in the stages at which the embryos were assayed.
23. M. C. Danos and H. J. Yost, *Dev. Biol.* **177**, 96 (1996).
24. J. L. Lohr, M. C. Danos, H. J. Yost, *Development* **124**, 1465 (1997).
25. D. Dufort, L. Schwartz, K. Harpal, J. Rossant, *ibid.* **125**, 3015 (1998).
26. T. King, R. S. Beddington, N. A. Brown, *Mech. Dev.* **79**, 29 (1998); P. G. Melloy *et al.*, *Dev. Biol.* **193**, 77 (1998).
27. C. Meno *et al.*, *Cell* **94**, 287 (1998).
28. Nodal expression was detected by X-Gal staining for β-Gal activity (*17*). Lefty and Pitx2 expression were detected by RNA in situ hybridzation (*16*). The probe that was used to detect Lefty expression (*15*) hybridizes to Lefty2 RNA, which is detected in the lateral plate mesoderm, and to Lefty1 RNA, which is detected in the prospective floor plate (ventral midline). Because Lefty1 RNA was not consistently detected in normal embryos, its absence in the mutant embryos is not considered significant.
29. We are grateful to E. Robertson and C. Chiang for $Ndl^{lacZ/+}$ and $Shh^{-/+}$ mice, respectively. We thank M. Kuehn, H. Hamada, and M. Blum for Nodal, Lefty, and Pitx2 probes, respectively, and J. Bristow and D. Goldman for helpful advice. We thank M. Embry and A. Gannon for technical assistance. We are also grateful to S. Strickland and our laboratory colleagues for critical readings of the manuscript. E.N.M. was supported by a Mentored Clinical Scientist Development award HD01216 from the NIH. This work was supported by NIH grant RO1 HD34380 (G.R.M.).

21 April 1999; accepted 18 June 1999

Bacterial Photoreceptor with Similarity to Photoactive Yellow Protein and Plant Phytochromes

ZeYu Jiang,[1] Lee R. Swem,[1] Brenda G. Rushing,[1] Savitha Devanathan,[2] Gordon Tollin,[2] Carl E. Bauer[1]*

A phytochrome-like protein called Ppr was discovered in the purple photosynthetic bacterium *Rhodospirillum centenum*. Ppr has a photoactive yellow protein (PYP) amino-terminal domain, a central domain with similarity to phytochrome, and a carboxyl-terminal histidine kinase domain. Reconstitution experiments demonstrate that Ppr covalently attaches the blue light–absorbing chromophore *p*-hydroxycinnamic acid and that it has a photocycle that is spectrally similar to, but kinetically slower than, that of PYP. Ppr also regulates chalcone synthase gene expression in response to blue light with autophosphorylation inhibited in vitro by blue light. Phylogenetic analysis demonstrates that *R. centenum* Ppr may be ancestral to cyanobacterial and plant phytochromes.

All photosynthetic organisms respond in some manner to light quality and quantity. Multicellular plants control development, floral induction, and phototropism through photoreceptors that absorb specific wavelengths of light. Algae, cyanobacteria, and anoxygenic photosynthetic bacteria control motility and gene expression in response to light.

Until recently, phytochrome was thought to be a plant- and algal-specific red and far-red light photoreceptor (*1*). However, the cyanobacteria *Synechocystis* and *Fremyella diplosiphon* have proteins with similarity to plant phytochromes (*2*). Plant and cyanobacterial phytochromes contain similar NH_2-terminal chromophore (bilin) binding domains as well as one or two COOH-terminal kinase domains (Fig. 1). Cyanobacterial phytochromes exhibit similarity to histidine sensor kinases (*2*). Plant phytochromes contain limited sequence similarity to histidine kinases, lacking some critical sequence motifs such as the highly conserved histidine residue of autophosphorylation (*3*). Nevertheless, plant phytochromes do undergo autophosphorylation, suggesting that they function as a sensor kinase in a signal transduction cascade (*4*).

Plant blue-light receptors cryptochrome CRY1, CRY2 (*5*), and NPH1 (*6*) contain flavin as chromophores. Cryptochromes exhibit similarity to photolyases, whereas NPH1 has similarity to serine kinases. Prokaryotic homologs of cryptochrome and NPH1 have

[1]Department of Biology, Indiana University, Jordan Hall, Bloomington, IN 47405, USA. [2]Department of Biochemistry, University of Arizona, Biosciences West Building, 1041 East Lowell Street, Post Office Box 210088, Tucson, AZ 85721, USA.

*To whom correspondence should be addressed. E-mail: cbauer@bio.indiana.edu

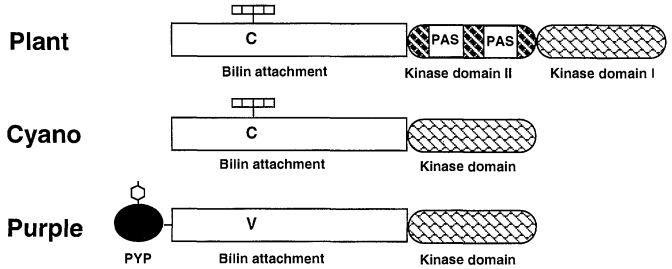

Fig. 1. Domains conserved among various phytochrome-like sequences.

not been described; however, many photosynthetic prokaryotes do contain a blue light–absorbing photoreceptor termed photoactive yellow protein (PYP) (*7*). PYP has the chromophore *p*-hydroxycinnamic acid attached by a covalent thioester linkage to a conserved cysteine (*8*). Blue-light excitation of PYP results in a reversible dark-light photocycle (*9*). High-resolution structural analyses of PYP in its ground state, as well as several photocycle intermediates, have been determined (*10*).

Despite detailed structural and biophysical knowledge of PYP, little is known of its biological role (*11*). To define a function for PYP, we cloned and disrupted a PYP homolog from the purple photosynthetic bacterium *Rhodospirillum centenum*, an organism that exhibits phototactic motility in response to blue light (*12*). Amplification of an internal domain of PYP by polymerase chain reaction (PCR) was accomplished with degenerate primers (*13*). Sequence analysis indicated that the amplified PYP domain was part of a much larger open reading frame encoding a ~96-kD polypeptide. A similarity (BLAST) search with the deduced polypeptide indicated the presence of a 135–amino acid PYP domain at the NH_2-terminus followed by a ~500–amino acid central domain with similarity to the chromophore (bilin) attachment domain of phytochromes (Fig. 1). The central domain is followed by a ~250–amino acid COOH-terminal domain with features typical of prokaryotic histidine kinases (*14*). Because of these structural features, we have named this gene *ppr* for PYP-phytochrome-related.

Alignment of the PYP domain of Ppr with PYPs from other bacteria showed high similarity, including the cysteine used for attachment of the chromophore *p*-hydroxycinnamic acid (Fig. 2A). Alignment of the middle domain with the bilin attachment domains from phytochromes shows that the conserved cysteine used for covalent attachment of bilin is absent (Fig. 2B). Indeed, the lack of the conserved bilin attachment cysteine in Ppr is congruent with the observation that anoxygenic photosynthetic bacteria do not synthesize linear tetrapyrroles. Thus, Ppr appears to have substituted the blue light–absorbing chromophore *p*-hydroxycinnamic acid in the PYP domain for red and far-red light–absorbing bilin that is attached to phytochromes.

We purified Ppr apoprotein and co-

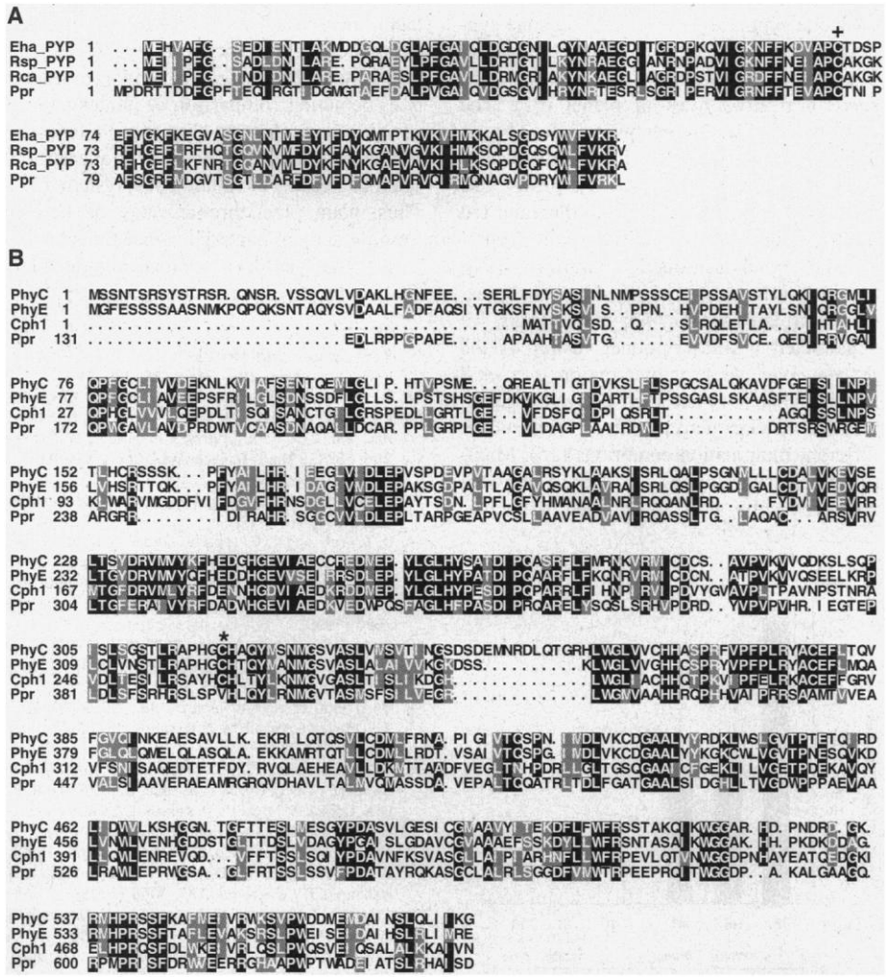

Fig. 2. DNA sequence alignments of *R. centenum* Ppr with selected PYP (**A**) and the bilin domains from phytochromes (**B**). Abbreviations in (A) are Eha_PYP, *Ectothiorhodospira halophila* PYP; Rsp_PYP, *Rhodobacter sphaeroides* PYP; Rca_PYP, *Rhodobacter capsulatus* PYP. Abbreviations in (B) are PhyC, phytochrome C from *Arabidopsis*; PhyE, phytochrome E from *Arabidopsis*; Cph1, phytochrome Cph1 from *Synechocystis* PCC6803. Conserved Cys residues used for chromophore attachment are indicated with a plus sign in the PYP domain and an asterisk in the phytochrome chromophore domain. Abbreviations for the amino acid residues are as follows: A, Ala; C, Cys; D, Asp; E, Glu; F, Phe; G, Gly; H, His; I, Ile; K, Lys; L, Leu; M, Met; N, Asn; P, Pro; Q, Gln; R, Arg; S, Ser; T, Thr; V, Val; W, Trp; and Y, Tyr.

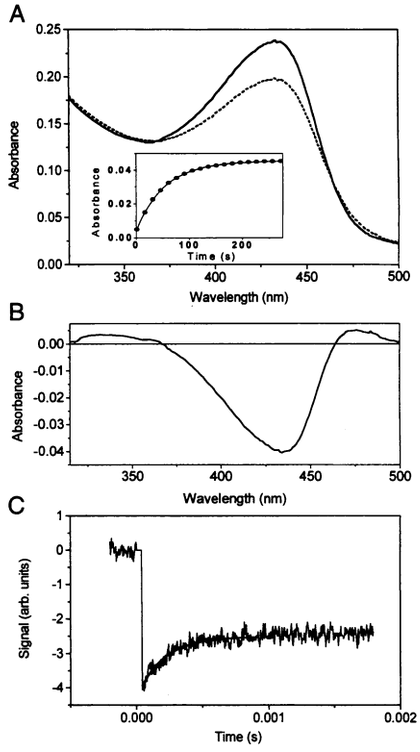

Fig. 3. Absorption characteristics of Ppr. (**A**) Absorption spectra of a dark-adapted Ppr (solid line) and the photobleached product (dashed line) obtained after 2 min of irradiation with a 40-W fiber optic lamp. (**Inset**) The kinetic trace observed during dark recovery of the 434-nm peak with 10-s data points. The line through the data points represents a single exponential fit with $k = 2.17 \times 10^{-2}\ s^{-1}$ (time constant = 46 s). (**B**) Light minus dark difference spectrum shows two spectral bands at 470 and 330 nm with isobestic points at 465 and 365 nm. (**C**) Microsecond laser flash photolysis transient observed at 434 nm after 445-nm excitation. Irradiation of Ppr resulted in a rapid loss of absorption with a biphasic recovery. The smooth line through the data is a single exponential fit to the partial fast recovery phase with $k = 4.7 \times 10^{3}\ s^{-1}$ (time constant = 1.5×10^{-4} s).

valently attached *p*-hydroxycinnamic acid using a procedure developed for PYP from *Ectothiorhodospira halophila* (*E*-PYP) (*15*). Reconstituted Ppr had a yellow color with an absorbance maximum at 434 nm (Fig. 3A). When irradiated with white light, steady-state photobleaching occurred followed by dark recovery with a time constant of 46 s (Fig. 3A). This recovery is 330-fold slower than that observed with *E*-PYP (*16*). The light minus dark difference spectrum indicated two spectral species, a red-shifted form at ~470 nm and a blue-shifted form at ~330 nm that have isosbestic points at 465 and 365 nm, respectively (Fig. 3B). These species are comparable to the I_1 and I_2 intermediates observed with *E*-PYP (*16*). A microsecond photolysis experiment by laser flash excitation at 445 nm resulted in a rapid decrease of the 434-nm absorbance followed by a fast partial recovery with a time constant of 0.21 ms (Fig. 3C). This was followed by a slow recovery component. The photocycle kinetics obtained with Ppr are different from those observed with *E*-PYP in which I_1 is formed with a time constant of 3 ns, I_2 with a time constant of 200 μs, and a return to the dark-adapted state in 140 ms (*16*).

In vitro kinase assays of both apoprotein and chromophore-reconstituted Ppr were performed under dark and light (400 to 900 nm) conditions to see if excitation affected kinase activity (*17*). Analysis of the apoprotein indicated that dark and illuminated kinase preparations had similar high rates of autophosphorylation (Fig. 4A). In contrast, the photochemically active reconstituted Ppr demonstrated two- to threefold higher phosphorylation under dark conditions than when illuminated as assayed after a 20-min incubation (Fig. 4, A and B). The inhibitory effect of light was reproducible and evident in four independent experiments (*18*). Because the apoprotein has kinase activity, the presence of significant amounts of apoprotein in these preparations (~40%) (*19*) tends to mask the inhibitory effect of light on the reconstituted protein.

We also assayed for a role of Ppr in phototaxis by the construction of a *ppr* deletion through allelic exchange with a spectinomycin cassette (*20*). The resulting strain exhibited no defects in photosensory behavior when compared with the wild-type parent strain (*18*). This indicates that a Ppr photosensory pathway does not interact with the chemotaxis sensory transduction cascade that governs photosensory behavior in this organism (*21*).

We next tested whether Ppr affects gene expression by assaying expression of the chalcone synthase gene (*chs*). Chalcone synthase is an early enzyme in the flavonoid biosynthetic pathway, the products of which serve protective roles in plants (*22*). The function of chalcone synthase in bacteria is unknown but it is present in several species, including *R. centenum* (*23*). In plants, *chs* expression is regulated by both blue and red light through the phytochrome and cryptochrome signal transduction pathways (*22*). Consequently, we tested whether *chs* expression is affected by Ppr. For these assays, we constructed a transcriptional fusion of the *R. centenum chs* promoter region to a *lacZ* reporter gene (*24*) and then assayed β-galactosidase (β-Gal) activity after growth under different illumination conditions (*25*). Maximal expression of *chs* was observed when wild-type cells were illuminated with only infrared light (Fig. 5). When these cells were illuminated with infrared light and white light, or infrared light and blue light (400 to 450 nm), *chs* expression was reduced twofold. Expression of *chs* is clearly dependent on Ppr as evidenced by low-level unregulated expression in the *ppr*-disrupted strain, C145. The finding that the *ppr*-deleted strain has much lower expression than the blue light–irradiated wild-type cells suggests that Ppr may be providing a certain basal level of phosphorylation to a signal transduction cascade under illuminated conditions that is ramped up to a higher level in the dark.

Given that *R. centenum* and plants both regulate chalcone synthase with related photoreceptors, it raises the intriguing question of whether Ppr is ancestral to phytochromes. For analysis we constructed a phylogenetic tree which indicated that bacterial phytochromes appear to be ancestral to plant phytochromes, with *R. centenum* phytochrome being the most distant (Web Fig. 6) (*18*, *26*). The phytochrome tree is similar to rooted trees depicting comparison of photosynthesis genes, which indicate that the photosystem synthesized by purple bacteria is ancestral to cyanobacterial and plant photosystem (*27*). Thus, plant phytochromes may be derived from an ancient bacterial signal transduction system that has been retained among many diverse photosynthetic organisms.

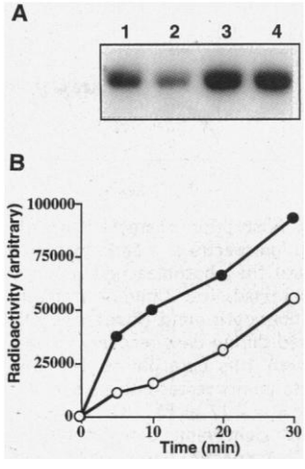

Fig. 4. Kinetics of autophosphorylation of Ppr when incubated with [γ -^{32}P]ATP (*17*). (**A**) Autoradiography of phosphorylated holoenzyme (lanes 1 and 2) and apoprotein (lanes 3 and 4) after a 20-min incubation in the dark (lanes 1 and 3) or in blue light (lanes 2 and 4). (**B**) Ppr autophosphorylation in reactions that were incubated in the dark (●) or that were illuminated with >400-nm light (○).

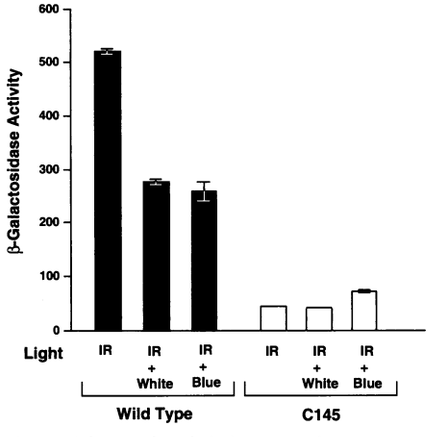

Fig. 5. Light-regulated chalcone synthase expression of a *chs::lacZ* fusion in wild-type and *ppr*-disrupted cells (strain C145). Cells were illuminated with infrared light (IR), IR + white light, or IR + blue light (400 to 450 nm) and measured for β-Gal activity (*25*). Activity units represent micromoles of *o*-nitrophenyl-β-D-galactopyranoside hydrolyzed min^{-1} mg^{-1} protein.

References and Notes

1. P. H. Quail, *Annu. Rev. Genet.* **25**, 389 (1991).
2. D. M. Kehoe and A. R. Grossman, *Science* **273**, 1409 (1996); K.-C. Yeh, S.-H. Wu, J. T. Murphy, J. C. Lagarias, *ibid.* **277**, 1505 (1997); J. Hughes *et al.*, *Nature* **386**, 663 (1997); T. D. Elich and J. Chory, *Cell* **91**, 713 (1997).
3. H. A. Schneider-Poetsch, *Photochem Photobiol.* **56**, 839 (1992).
4. K. C. Yeh and J. C. Lagarias, *Proc. Natl. Acad. Sci. U.S.A.* **95**, 13976 (1998).
5. M. Ahmad and A. R. Cashmore, *Nature* **366**, 162 (1993); C. Lin *et al.*, *Proc. Natl. Acad. Sci. U.S.A.* **95**, 2686 (1998).
6. J. M. Christie *et al.*, *Science* **282**, 1698 (1998).
7. T. E. Meyer, *Biochim. Biophys. Acta* **806**, 175 (1985); R. Kort *et al.*, *EMBO J.* **15**, 3209 (1996).
8. W. D. Hoff *et al.*, *Biochemistry* **33**, 13959 (1994).
9. T. E. Meyer, E. Yakali, M. A. Cusanovich, G. Tollin, *ibid.* **26**, 418 (1987).
10. G. E. O. Borgstahl, D. R. Williams, E. D. Getzoff, *ibid.* **34**, 6278 (1995); P. Dux *et al.*, *ibid.* **37**, 12689 (1998); U. K. Genick, S. M. Soltis, P. Kuhn, I. L. Canestrelli, E. D. Getzoff, *Nature* **392**, 206 (1998); T. E. Meyer, G. Tollin, M. A. Cusanovich, *Science* **281**, 1964 (1998).
11. W. W. Sprenger, W. D. Hoff, J. P. Armitage, K. J. Hellingwerf. *J. Bacteriol.* **175**, 3096 (1993).
12. L. Ragatz, Z. Y. Jiang, C. E. Bauer, H. Gest, *Nature* **370**, 104 (1994); *Arch. Microbiol.* **163**, 1 (1995).
13. PYP-phytochrome was amplified by PCR with oligonucleotides GTSATCGGNAAGAACTTCTTY and ACSCGYTTSACGAANANCCA. The entire gene was cloned from a genomic library, sequenced, and deposited in GenBank database under accession number AF064527.
14. J. S. Parkinson and E. C. Kofoid, *Annu. Rev. Genet.* **26**, 71 (1992).
15. The *ppr* gene was amplified by PCR with primers GGATTACCATATGCCGGACCGGACCACCGAC and CGAATTCTCAGGCCCCGATCTCGATGG, and cloned into Nde I and Eco RI sites of pET28a(+) (Novagen).

Escherichia coli–expressed Ppr was purified (~85% pure) on a HiTrap metal-chelating column (Pharmacia). Ppr was dialyzed and stored at −80°C in 400 mM KCl, 50 mM tris-HCl (pH 7.9), 10 mM $MgCl_2$, 0.1 mM EDTA, and 50% glycerol. *p*-Hydroxycinnamic acid was attached as described [S. Devanathan *et al.*, *Arch. Biochem. Biophys.* **340**, 83 (1997)].

16. T. E. Meyer, G. Tollin, J. H. Hazzard, M. A. Cusanovich, *Biophys. J.* **56**, 559 (1989); T. E. Meyer, G. Tollin, T. P. Causgrove, P. Cheng, R. E. Blankenship, *ibid.* **59**, 988 (1991); L. Ujj *et al.*, *Biophys. J.* **75**, 406 (1998).
17. Samples containing 60 μg of protein were diluted with storage buffer (*15*) to a volume of 288 μl. Half of the reaction mixture was incubated in the dark and the other in >400-nm light (5.5 mW/cm²) for 30 min at room temperature. [γ-^{32}P]ATP mix {1.0 mM adenosine 5′-triphosphate (ATP) and 0.024 mM [γ -^{32}P] ATP (7000 Ci/mmole, ICN)} was added to initiate the reactions. Partitions of 12 μl (2.5 μg of protein) were removed at time intervals, mixed with SDS–loading buffer, and placed on ice. The samples were later fractionated by SDS–polyacrylamide gel electrophoresis. ^{32}P-Labeled protein bands were quantified by PhosphorImager analysis (Molecular Dynamics, Sunnyvale, CA).
18. Z. Jiang and C. E. Bauer, unpublished data.
19. The extinction coefficient of Ppr at 280 nm was 101,820 M^{-1} cm^{-1} and that of *p*-hydroxycinnamate was 45,000 M^{-1} cm^{-1}, so the maximum ratio of absorption of Ppr at 434 nm to that at 280 nm is 0.442. The ratio of absorption of reconstituted Ppr at 434 nm to that at 280 nm was 0.29, giving a ~60% efficiency of attachment (*7*).
20. *ppr* amino acid residues 114 to 750 were replaced with a spectinomycin resistance gene in the suicide vector pGmLacZ. After delivery by conjugation (*21*), double recombinants were selected and confirmed by PCR analysis.
21. Z. Y. Jiang, H. Gest, C. E. Bauer, *J. Bacteriol.* **179**, 5720 (1997).
22. C. R. Martin, *Int. Rev. Cytol.* **147**, 233 (1993).
23. GenBank Accession number AF121274.
24. The *R. centenum chs* promoter was amplified by PCR with primers TAGGTACCGATGAACAGCCAGGCGAG and TAGCATGCCGTGAAAACGGGGGAGAG. The PCR product was cloned into the *lacZ* reporter plasmid pZJD11 (*21*) and maintained with antibiotics.
25. *R. centenum* was cultured in peptone–yeast extract–soytone (*12*) and illuminated with infrared light (>700 nm). White light was provided with a 400-W pressure sodium Lumalux lamp (LU400, Osram Sylvania, Danvers, MA) and blue light (400 to 450 nm) by passing the white light through filters. Cells were assayed for β-Gal activity as described (*21*).
26. Supplemental Web material is available at www.sciencemag.org/feature/data/1039035.shl.
27. J. K. Xiong, K. Inou, C. E. Bauer, *Proc. Natl. Acad. Sci. U.S.A.* **95**, 14851 (1998).
28. We thank T. Meyer and R. Hangarter for comments. Supported by NIH grant GM 40941 (C.E.B.) and a NSF postdoctoral fellowship (B.G.R.).

3 February 1999; accepted 14 June 1999

An Allele of *COL9A2* Associated with Intervertebral Disc Disease

Susanna Annunen,[1] Petteri Paassilta,[1] Jaana Lohiniva,[1] Merja Perälä,[1] Tero Pihlajamaa,[1] Jaro Karppinen,[2] Osmo Tervonen,[3] Heikki Kröger,[5] Seppo Lähde,[3] Heikki Vanharanta,[2] Lasse Ryhänen,[4] Harald H. H. Göring,[6] Jürg Ott,[6,7] Darwin J. Prockop,[8] Leena Ala-Kokko[1,8]*

Intervertebral disc disease is one of the most common musculoskeletal disorders. A number of environmental and anthropometric risk factors may contribute to it, and recent reports have suggested the importance of genetic factors as well. The *COL9A2* gene, which codes for one of the polypeptide chains of collagen IX that is expressed in the intervertebral disc, was screened for sequence variations in individuals with intervertebral disc disease. The analysis identified a putative disease-causing sequence variation that converted a codon for glutamine to one for tryptophan in six out of the 157 individuals but in none of 174 controls. The tryptophan allele cosegregated with the disease phenotype in the four families studied, giving a lod score (logarithm of odds ratio) for linkage of 4.5, and subsequent linkage disequilibrium analysis conditional on linkage gave an additional lod score of 7.1.

Intervertebral disc disease is among the most common musculoskeletal disorders. It is a major cause of work disability and an extremely costly health care problem. It is typically associated with sciatica, which has a prevalence of about 5% in Finland (*1*). Sciatica is defined as pain caused by a lesion of the spinal nerve root radiating along the femoral or sciatic nerve from the back into the dermatome of the root. It is usually related to either disc protrusion or herniation, which will cause both chemical and mechanical irritation of the nerve root. Even though there is an association between various environmental and anthropometric risk factors and sciatica, their effects are modest (*2, 3*). A recent twin study suggests that genetic factors may be involved in the pathogenesis of intervertebral disc disease and sciatica (*3*). This is supported by findings of a considerable genetic predisposition to early-onset sciatica and lumbar disc herniation in certain families (*4*). Therefore, intervertebral disc disease appears to be similar to other common complex diseases with multiple genetic forms and a high phenocopy rate, such as breast cancer and Alzheimer's disease.

Intervertebral discs contain an abundant extracellular matrix of proteoglycans and collagens (*5*). The outer layer, the annulus fibrosus, consists mainly of collagen I, and the interior structure of the disc, the nucleus pulposus, is about 50% proteoglycan, mainly aggrecan, and 20% collagen II. Both contain small amounts of collagen IX. Recent results indicate that mutations in collagen IX and aggrecan can cause age-related disc degeneration and herniation in mice (*6, 7*).

Collagen IX is a heterotrimer of three α chains, α1(IX), α2(IX), and α3(IX), encoded by the genes *COL9A1*, *COL9A2*, and *COL9A3*, respectively. It consists of three collagenous (COL1 to COL3) and four noncollagenous (NC1 to NC4) domains (*8*). The COL2 domain is covalently linked to collagen II fibrils (*9*). Collagen IX is thought to serve as a bridge between collagens and noncollagenous proteins in tissues.

To study the role of collagen IX in intervertebral disc disease and associated sciatica, we selected 157 unrelated Finnish individuals (ages 19 to 78; mean = 44, SD = 13) with unilateral pain of duration over 1 month radiating from the back to below the knee (dermatomes L4, L5, and S1). Therefore, the subjects had the most characteristic symptom of herniated intervertebral disc (*1*). After clinical evaluation, 156 of them were examined by magnetic resonance imaging (MRI) and one was evaluated by computerized tomography (CT) (*10*). Radiologically detectable intervertebral disc disease was present at the time of the examination in 73% of the cases. Initially, *COL9A2* was screened for sequence variations by conformation-sensitive gel electrophoresis (CSGE) in 10 patients (*11*), yielding a unique CSGE pattern in the polymerase chain reaction (PCR) products for exon 19 in one case (Fig. 1). Sequencing (*12*) indicated a

Fig. 1. CSGE analysis of exon 19 of the *COL9A2* gene. The exon and its flanking sequences were amplified by PCR from the proband (P) and a control (C) using primers specific for intron 18 (5′-TGGATCT-CAGTTTCCCTACCTG, −92 to −71 in infron 18) and infron 19 (5′-CAAGAGGTGGTGATT-GAGCAAGAGC, +99 to +75 in infron 19). The analysis indicated heteroduplexes in the proband's sample.

[1]Collagen Research Unit, Biocenter and Department of Medical Biochemistry; [2]Department of Physical Medicine and Rehabilitation; [3]Diagnostic Radiology; [4]Internal Medicine, University of Oulu, 90220 Oulu, Finland. [5]Department of Surgery, University of Kuopio, 70211 Kuopio, Finland. [6]Department of Genetics and Development, Columbia University, New York, NY 10032, USA. [7]Laboratory of Statistical Genetics, Rockefeller University, New York, NY 10021, USA. [8]Center for Gene Therapy, MCP Hahnemann University, Philadelphia, PA 19102, USA.

*To whom correspondence should be addressed (in Finland). E-mail: leena.ala-kokko@oulu.fi